
FLEdge: Benchmarking Federated Machine Learning Applications in Edge Computing Systems

Herbert Woisetschläger*
Technical University of Munich
Germany
herbert.woisetschlaeger@tum.de

Alexander Isenko
Technical University of Munich
Germany
alex.isenko@tum.de

Ruben Mayer
University of Bayreuth
Germany
ruben.mayer@uni-bayreuth.de

Hans-Arno Jacobsen
University of Toronto
Canada
jacobsen@eecg.toronto.edu

Abstract

Federated Machine Learning (FL) has received considerable attention in recent years. FL benchmarks are predominantly explored in either simulated systems or data center environments, neglecting the setups of real-world systems, which are often closely linked to edge computing. We close this research gap by introducing FLEdge, a benchmark targeting FL workloads in edge computing systems. We systematically study hardware heterogeneity, energy efficiency during training, and the effect of various differential privacy levels on training in FL systems. To make this benchmark applicable to real-world scenarios, we evaluate the impact of client dropouts on state-of-the-art FL strategies with failure rates as high as 50%. FLEdge provides new insights, such as that training state-of-the-art FL workloads on older GPU-accelerated embedded devices is up to 3x more energy efficient than on modern server-grade GPUs.

1 Introduction

Federated Learning (FL) has become an established technique for distributed and privacy-preserving deep learning (DL). With increasing access to data by eliminating the necessity of transferring data to a central location, FL not only reduces network communication but also fosters privacy. There is ample research on benchmarking FL applications, which focuses on different fields of application, data heterogeneity [1, 2], FL aggregation strategies [2, 3], DL model personalization [4], and federated hyperparameter optimization [5]. However, these benchmarks are typically evaluated on server-grade hardware. As such, an often neglected factor is the type of system FL applications are deployed to: Edge computing systems.

Edge computing is a pattern for managing a fleet of devices distributed across geographies [6], serving latency-critical or data-sensitive tasks [7, 8]. While typically used together with cloud services, low-power embedded devices are located closest to the data source and therefore serve as the data processing unit in FL systems. Embedded devices have mostly been regarded as data pass-through gateways, not requiring them to have powerful hardware [9]. As such, the majority of machines found in real systems are not optimized for DL workloads. This is especially true for industrial applications. There, systems are often comprised of hardware released 5+ years ago without any hardware acceleration [10, 11], originating from high functional safety requirements and long

*Corresponding author

product lifecycles. Aside from computational limitations, edge computing systems are confronted with additional challenges. Since devices are often mobile or embedded, processing power, energy consumption, and resource availability are key concerns [12, 13]. While devices addressing these limitations exist [14, 15], there are no comprehensive guidelines on which system to use for FL.

Even though there are various considerations for incorporating hardware heterogeneity into FL applications [16, 17, 18], there is no standardized benchmark for evaluating critical design factors of FL applications in edge computing systems. As such, we identify four key challenges:

- (1) **Under-representation of hardware heterogeneity.** Current research focuses on evaluating FL methods and model architectures in scalable data center environments without taking into account real-world edge computing hardware requirements. This results in significant performance differences when deploying on heterogeneous hardware and limits the applicability to edge computing systems [19, 2, 6].
- (2) **Diverse energy efficiency metrics.** Currently, the effects of FL methods are evaluated either on power estimation based on compute cycles [19] or the amount of FLOPS required to complete a task [4]. Oftentimes these results are not comparable as they are specific to the underlying computing architecture, such as x86 or ARM. x86 is typically found in data center hardware [20] while ARM is built for mobile applications [21].
- (3) **Under-explored client dropout robustness.** Many benchmarks for FL applications provide a variety of DL models and datasets along with various FL strategies [2, 1]. Yet, there is no work that systematically studies the effects of client dropouts on overall learning performance. Client dropouts are likely to happen in edge computing systems where both clients and network connectivity can be unstable.
- (4) **Separation of FL methods and differential privacy in evaluations.** FL already provides improvements w.r.t. data privacy. Yet, there are multiple studies that find federally trained models to be vulnerable to membership inference attacks [22, 23]. Oftentimes, new FL methods are evaluated without consideration of privacy-enhancing methods such as differential privacy (DP), required to provide the necessary level of privacy.

To address these key challenges, we create a uniform framework for exploring new FL methods and DL models in edge computing systems. We help practitioners to evaluate FL deployments in hardware-heterogeneous environments under consideration of energy efficiency, client reliability, and data privacy. Our contributions are as follows:

- (1) **We introduce FLEdge - a comprehensive benchmarking suite for FL applications in hardware-heterogeneous environments.** The benchmark is available with an open-source code base.² It does not only include a set of reference implementations for datasets from the CV [1], NLP [2], and NILM [24] domains but also tools to holistically capture systems metrics (incl. energy consumption). Through its modular design, our benchmark is easily extensible with additional datasets and models.
- (2) **We evaluate widely used embedded devices,** compare their performance on various FL applications, and identify computational limitations that can have significant effects on the performance of FL methods. Our results reveal that hardware-accelerated embedded devices are up to 3x more energy-efficient for the evaluation of state-of-the-art FL applications than modern data center GPUs. As such, we find a discrepancy between the typical evaluation environment for novel FL methods and the actual field of application.
- (3) **We systematically conduct experiments on various state-of-the-art FL strategies and their robustness against client dropouts** during training rounds with dropout rates of up to 50%. We find that there is no such thing as a one strategy fits all solution. Yet, for each dataset, we identify one strategy that consistently performs best across different client dropout rates.
- (4) **We evaluate the effects of user-level DP on global model performance,** which is a de-facto requirement for providing sufficient levels of privacy to users. Our results show that we generally lose approximately 10 percentage points as compared to training without DP when introducing loose privacy guarantees. For tighter privacy guarantees, the accuracy still diminishes, yet to an insignificant degree.

²Code is available on GitHub under Apache 2.0 license: <https://github.com/laminair/FLEdge> .

Our work is structured as follows. Section 2 will introduce related work and Section 3 will outline relevant background. In Section 4, we present our benchmark design including datasets, DL models, and FL strategies. Section 5 contains experimental evaluations of our benchmark. In Section 6, we conclude our work.

2 Related Work

We divide our related work section into two parts: DL in edge computing systems and FL benchmarks. **Edge computing.** For Edge Computing systems there are numerous benchmarking tools. Edge devices have long been regarded as a data pass-through gateway rather than data processing devices and therefore have been evaluated in the context of data transfer capacities and reliability [25]. In 2019, McChesney et al. [26] introduced DeFog, a benchmark including DL inference workloads on embedded devices with YOLO models. Yet, these benchmarks do not include system dependencies between clients and a server as we would find in FL systems, where training progress relies on client participation. Varghese et al. [27] provide a comprehensive overview of a wide range of edge computing benchmarks, but none of them is targeted to FL.

FL benchmarks. The benchmarking landscape for FL applications is manifold. While there is a set of general purpose FL benchmarks like LEAF [1], FedML [2], or FedScale [3] that provide a basis for exploring DL workloads with different FL strategies, the attention of researchers is moving towards use-case-specific benchmarks. For instance, pFL-Bench [4] provides a basis for exploring and building personalized FL applications while FedHPO-B [5] is a benchmark targeting federated hyperparameter optimization. Each of these benchmarks targets a very specific type of application or domain, while there is little research on hardware heterogeneity and real-world scenarios. With FLEdge, we close this gap by providing an application-agnostic benchmark for evaluating data and device heterogeneity along with client dropouts and differentially private workloads.

3 Background

As edge computing applications are gaining in popularity, especially in environments without perfect control over system parameters, challenges in designing efficient systems arise. These challenges involve competition for resources between multiple tasks, data collection schedules on edge devices, and external effects on an edge client’s overall availability. In the context of this work, we aim to quantify the effects these challenges have on FL applications in edge computing systems.

Hardware heterogeneity. Edge computing is designed around the pattern of offloading computational tasks to edge devices, usually embedded devices in the proximity of a data source. This provides better control over processing latency [28]. Yet, a major challenge in these systems is hardware heterogeneity, either due to long product life cycles in industrial systems controlled by a small number of entities or due to a lack of infrastructure control in systems with a large number of participants. For instance, widely used embedded devices for industrial edge require extensive testing for reliability and are therefore including hardware as old as 5 years [11]. As such, deployment of FL applications will likely happen on heterogeneous hardware with greatly varying computational capabilities. Oftentimes, this capability variation introduces challenges in deploying a DL model for training, even without FL [29].

Energy efficiency. Typically, embedded devices are used in edge computing systems to facilitate data collection. Yet, for FL applications these devices are now required to run computationally intensive workloads. This results in increased energy consumption, which is often a challenge due to limited power availability [30]. To mitigate these effects, hardware acceleration on embedded devices has been introduced [15]. For instance, for typical DL GPUs generally provide a significant performance benefit over CPUs while being more energy efficient and cost-saving at the same time [31]. Therefore, it is essential to investigate the efficiency of different hardware w.r.t. their projected workloads.

System robustness. Reliability is key for an application. While for the majority of edge computing applications tasks are running individually on clients, e.g., in the context of CV applications with MobileNet models [32], for FL there are significant dependencies between clients and the server. Training in FL systems happens over multiple rounds $t \in T$ with a total of N clients in the system while $M \in N$ is the number of clients sampled in a training round, assuming the same number of clients throughout. Training an FL model involves aggregating multiple client updates into

a single model. The basic procedure is described with $w^{t+1} = \frac{1}{M}(\sum_{m \in M} w_m^t)$. Since edge computing systems can suffer from client dropouts due to hardware or network failures this implies for FL systems that $|M|$ varies between training rounds. Consequently, fewer client updates will be aggregated.

Data privacy. Another key concern for FL systems is data privacy as clients are not willing to share their data. FL already increases the level of data privacy to a certain extent [33] but does not provide a *guarantee* for privacy to clients. To obtain such a guarantee, formal methods like (ϵ, δ) -Differential Privacy (DP) can be applied. DP can either be applied on sample- or user-level, where the latter is of special interest for FL [34, 35]. As clients in FL systems only share their model updates, it is sufficient to apply DP to DL model updates and achieve the same guarantees as with sample-level DP [36]. The objective of user-level DP is to deny inference of input data a client used for training their local model. For user-level DP, the model aggregation method is extended by adding Gaussian noise to the model weights $w^{t+1} = \frac{1}{M}(\sum_{m \in M} w_m^t + z * \mathcal{N}(0, I\sigma_{\Delta}^2))$. With the additional noise \mathcal{N} , we introduce a natural trade-off between model accuracy and the level of privacy. σ_{Δ}^2 depends on the number of clients sampled in a training round and on their L2 update norm, as with more heterogeneous client updates more noise has to be added to ensure (ϵ, δ) -DP. The privacy strength of the privacy guarantee is measured by the privacy budget ϵ where lower values are better and provide higher levels of privacy [37]. ϵ depends on δ , the likelihood of unintentional input data leakage. Usually, δ is set to a value lower than the inverse of the total number of samples in a dataset.

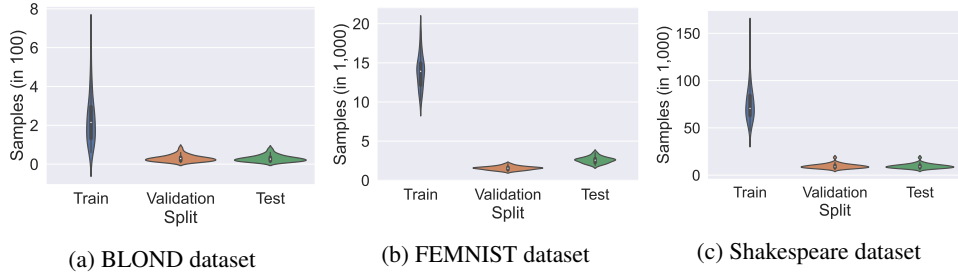


Figure 1: Distribution of client subset sizes across the datasets used in this paper. The datasets were split by sampling from a Dirichlet distribution ($\alpha = 1$).

4 Benchmark Design

Our benchmark focuses on widely used state-of-the-art datasets from the NILM, CV, and NLP domains for FL applications. For NILM, we use the BLOND dataset [24]. It is an office environment appliance load monitoring dataset. It contains 13,164 samples with 12 appliance classes [38]. We employ the FEMNIST dataset [1] for CV. FEMNIST consists of 814,000 samples of hand-written digits and letters. We use the Shakespeare dataset [2] for NLP. The dataset consists of William Shakespeare’s complete work. We use it to perform next character prediction on 4,200,000 samples. In total, our vocabulary contains 80 tokens representing letters, digits, and special characters.

4.1 Datasets, DL Models, and FL Strategies

Datasets. Researching FL applications on physical devices usually requires fitting the data distribution to the number of devices in a testbed. As our edge computing testbed contains 45 embedded devices, we opt to sample client subsets based on a Dirichlet distribution ($\alpha = 1$) to fit the number of clients in our testbed (Figure 1). Full details on the datasets are available in Appendix A.1.

Models. We train a total of 6 DL models in total. For FEMNIST, we adopt the widely used CNN architecture presented in the LEAF benchmark [1]. For Shakespeare, we adopt the LSTM and fully connected layer architecture from the FedML benchmark [2]. For BLOND, we use four different models, a CNN, an LSTM, a ResNet, and a DenseNet architecture [38]. For all six models, we train one local epoch on clients and then send updates for aggregation to the server to eliminate potential risks of client drift [33]. The exact hyper-parameterization of all models is available in Appendix A.2.

FL Strategies. We explore all models in conjunction with 6 state-of-the-art FL strategies. We include FedAvg, the first communication-efficient FL strategy, which aggregates client updates over an

unweighted average [33]. We also include adaptive strategies introduced by Reddi et al. [39], namely FedAdam, FedYogi, and FedAdaGrad. The adaptive strategies introduce a server-side learning rate to better account for data heterogeneity. We further adopt two strategies that aim to increase fairness and robustness in an FL system. FedProx [40] introduces a method for weighting client updates in the aggregation process based on the amount of data a client has processed for an update. q-fair FedAvg (qFedAvg) [41] is a derivative of FedAvg introducing a factor q that determines the level of fairness. Fairness in this context is defined by how well a model generalizes across clients. Higher generalizability is achieved by overweighting those clients that have the highest loss. This is done to gear a model stronger towards the high-loss clients and reduce the accuracy variance across clients. Further details on the datasets and DL models are available in Appendix A.

4.2 Benchmark Scenarios & Evaluation Criteria

We evaluate all workloads in light of edge computing systems that train on heterogeneous hardware and suffer from instabilities.

Hardware heterogeneity. To evaluate the training performance of various device types, we perform a microbenchmark measuring the average time it takes to complete training on a single minibatch of data. For this, we specifically evaluate the data-loading, forward, loss calculation, backward, and optimizer step times of all DL models. We aim at identifying the point where training on low-power embedded devices like Raspberry Pi 4 becomes impractical.

Energy efficiency. Based on the microbenchmark, we measure the real-time power draw (in Watt) and put it into context with the training throughput measured in samples per second (SPS). We define the energy efficiency of a device as $\eta_e = \frac{SPS}{W}$.

Client dropouts during training rounds. As FL strategies are usually evaluated under perfect conditions, we evaluate all DL model and FL strategy combinations under gradually increasing client dropout levels from 0% to 50% per training round. Dropped-out clients can re-register at the server and participate again in later training rounds, as it would happen in real-world scenarios. We train with 45 clients over 10 rounds.

Differentially private workloads. We employ (ϵ, δ) -DP with adaptive weight clipping [34, 35]. We introduce user-level DP by adding z-modulated Gaussian noise to the DL model weights on the server side in each training round. Throughout these experiments, we report the privacy budget spent (ϵ) after 10 rounds of training. We set the likelihood of unintentional data leakage $\delta = 1/n$ with n being the number of total samples in a dataset across all clients, e.g., $n = 13, 164$ for the BLOND dataset.

4.3 Device Configurations & Code Availability

We aim to explore FL applications in real systems by introducing four different device types. As a baseline, we use a GPU-accelerated data center node with 64 CPU cores, 256 GB of memory, and an NVIDIA A6000 (GPU). As a proxy for x86-based embedded devices without hardware acceleration, we use virtualized systems with 4 CPU cores and 4 GB of memory (VM). For embedded devices, we use Raspberry Pi 4B (RPi) devices with 4 GB of memory and NVIDIA Jetson Nano 2 GB modules (Nano) with 128 NVIDIA Maxwell GPU cores. To measure the real-time energy consumption during our experiments, we connected all embedded devices via PoE+ [42] and monitor the energy consumption via the network switches with 1 Hz. Further details on the software stack and implementation of energy monitoring are available in Appendix B.1. FLEdge is designed with open access and modularity in mind. We open-source our entire code base and all dataset splits we use in our experiments. As the basis for our FL system, we use Flower [19], which offers a flexible backend for client-server communication. To simplify adding new DL models and datasets, we opted for PyTorch Lightning [43], which offers a standardized API for configuring end-to-end DL pipelines with PyTorch.

5 Evaluation

To show the practical utility of FLEdge, we run extensive experiments on hardware heterogeneity, energy efficiency, client dropouts, and differentially private workloads. In this section, we present the

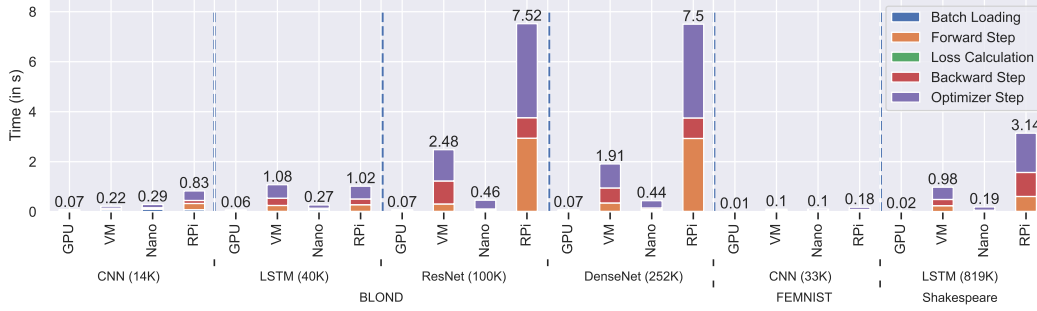


Figure 2: Training times for different device types and model sizes over one minibatch. Next to the model name, we report the model parameters. Lower is better. A full comparison of timings between the device types is available in Appendix C.1.

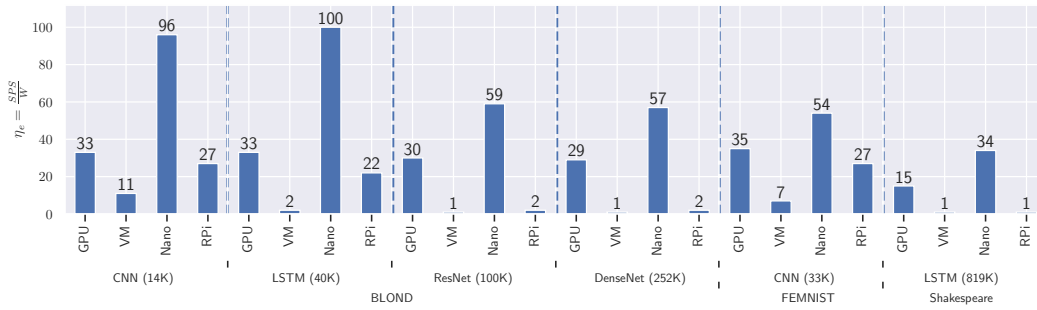


Figure 3: Sample efficiency measured across datasets and DL models (# parameters).³Results are measured over one epoch of training. Higher values are better.

main results and key insights while in Appendix C we provide supplementary evaluations and system metrics.

5.1 Hardware Heterogeneity

Embedded devices without hardware acceleration struggle with models larger than 100K parameters. The forward step time is the biggest improvement of Nanos vs the RPi which was up to 6x, 8x, 100x, and 66x times faster for the CNN, LSTM, ResNet, and DenseNet models, respectively, when training on the BLOND dataset (Figure 2). Similar patterns are observable for the FEMNIST CNN and the Shakespeare LSTM, where the forward step is 11x and 28x faster on the Nanos vs. the RPi. For the 100K+ parameter models, the forward step times are in the range of 10 milliseconds on the Nanos but they are well above one second for the RPi.

While the backward and optimizer steps played a slightly lesser role, the backward step was up to 20x lower on the Nanos vs. the RPi when training on BLOND. The optimizer step time is up to 13x lower on the BLOND models. The trend is similar for the FEMNIST and Shakespeare models, where the backward step times are 4x and 42x lower, respectively. The optimizer step times on the Nanos are 1.5x and 12x below the RPi times. All of these reduced training times on the Nanos by a total of 3x, 4x, 16x, and 17x compared to the RPi and even beat the x86 VM in all models except the BLOND CNN due to its small parameter count. To summarize, as the model size increases, the effects of hardware acceleration on the Nanos eclipse non-hardware accelerated embedded devices, and even trump the significantly more powerful x86 VMs. This makes them a high value proposition, even if their hardware is already 4 years old. Furthermore, the different performance characteristics of embedded devices may have significant effects on the applicability of DL model personalization [4] or hyperparameter optimization methods [5] in FL systems. Full details on the speedup statistics are available in Appendix C.1.

³We use estimates from SelfWatts [44] for approximating the power consumption of VMs.

Table 1: Global model accuracy across FL strategies with varying client dropout rates after 10 FL training rounds with a client selection rate of 20% per training round. The accuracy is tested with the global test split of each dataset. **Bold** highlights the best-performing FL strategy.

| Dropout | Strategy | BLOND | | | | FEMNIST | Shakespeare |
|-----------------------------|------------|------------------|------------------|------------------|------------------|------------------|------------------|
| | | CNN | DenseNet | LSTM | ResNet | CNN | LSTM |
| Local Baseline (no dropout) | N/A | 0.96±0.02 | 0.89±0.01 | 0.95±0.01 | 0.91±0.01 | 0.75±0.02 | 0.59±0.01 |
| 0% | FedAdaGrad | 0.76±0.0 | 0.17±0.07 | 0.71±0.03 | 0.70±0.0 | 0.56±0.01 | 0.52±0.01 |
| | FedAdam | 0.73±0.01 | 0.03±0.0 | 0.64±0.05 | 0.64±0.02 | 0.38±0.05 | 0.5±0.03 |
| | FedAvg | 0.75±0.02 | 0.74±0.0 | 0.77±0.01 | 0.73±0.01 | 0.7±0.0 | 0.53±0.0 |
| | FedProx | 0.75±0.01 | 0.74±0.0 | 0.74±0.01 | 0.73±0.01 | 0.7±0.0 | 0.52±0.0 |
| | FedYogi | 0.8±0.01 | 0.79±0.0 | 0.81±0.01 | 0.78±0.0 | 0.53±0.0 | 0.25±0.0 |
| | qFedAvg | 0.73±0.0 | 0.7±0.0 | 0.79±0.0 | 0.71±0.0 | 0.03±0.0 | 0.47±0.0 |
| 10% | FedAdaGrad | 0.76±0.03 | 0.03±0.0 | 0.69±0.02 | 0.68±0.02 | 0.55±0.04 | 0.51±0.02 |
| | FedAdam | 0.73±0.01 | 0.03±0.0 | 0.54±0.1 | 0.41±0.22 | 0.35±0.01 | 0.48±0.01 |
| | FedAvg | 0.7±0.04 | 0.73±0.01 | 0.69±0.04 | 0.72±0.0 | 0.69±0.01 | 0.52±0.01 |
| | FedProx | 0.74±0.05 | 0.73±0.01 | 0.68±0.03 | 0.73±0.01 | 0.68±0.01 | 0.52±0.01 |
| | FedYogi | 0.76±0.02 | 0.78±0.01 | 0.8±0.0 | 0.76±0.03 | 0.53±0.01 | 0.23±0.01 |
| | qFedAvg | 0.73±0.0 | 0.69±0.0 | 0.77±0.0 | 0.71±0.0 | 0.03±0.0 | 0.47±0.0 |
| 20% | FedAdaGrad | 0.64±0.1 | 0.04±0.0 | 0.48±0.3 | 0.69±0.03 | 0.49±0.06 | 0.49±0.02 |
| | FedAdam | 0.73±0.0 | 0.03±0.0 | 0.53±0.13 | 0.63±0.0 | 0.34±0.05 | 0.35±0.06 |
| | FedAvg | 0.32±0.27 | 0.69±0.05 | 0.74±0.03 | 0.72±0.01 | 0.68±0.02 | 0.51±0.02 |
| | FedProx | 0.37±0.3 | 0.69±0.05 | 0.68±0.04 | 0.72±0.01 | 0.67±0.01 | 0.51±0.02 |
| | FedYogi | 0.76±0.02 | 0.76±0.03 | 0.76±0.0 | 0.75±0.03 | 0.47±0.08 | 0.21±0.03 |
| | qFedAvg | 0.72±0.01 | 0.68±0.0 | 0.75±0.0 | 0.71±0.0 | 0.03±0.0 | 0.47±0.0 |
| 50% | FedAdaGrad | 0.42±0.24 | 0.03±0.0 | 0.35±0.27 | 0.68±0.04 | 0.45±0.06 | 0.45±0.03 |
| | FedAdam | 0.25±0.25 | 0.03±0.0 | 0.18±0.13 | 0.62±0.01 | 0.2±0.09 | 0.35±0.02 |
| | FedAvg | 0.46±0.16 | 0.67±0.06 | 0.66±0.01 | 0.7±0.02 | 0.66±0.03 | 0.49±0.03 |
| | FedProx | 0.52±0.16 | 0.67±0.06 | 0.68±0.04 | 0.7±0.02 | 0.64±0.02 | 0.49±0.03 |
| | FedYogi | 0.72±0.01 | 0.71±0.09 | 0.74±0.04 | 0.74±0.04 | 0.43±0.12 | 0.2±0.04 |
| | qFedAvg | 0.68±0.01 | 0.67±0.0 | 0.72±0.01 | 0.71±0.0 | 0.03±0.0 | 0.47±0.0 |

5.2 Energy Efficiency

Hardware accelerated embedded devices excel in the evaluation of FL applications. Overall, we find the Nanos to be the most energy-efficient device in our testbed. Comparing the Nanos to the RPis, we find the Nanos to be 3x more energy efficient (Figure 3) for the BLOND CNN. For the other BLOND models η_e is up to 25x higher compared to the RPis. For FEMNIST, the Nanos η_e is 2x higher than for the RPis. For Shakespeare, η_e for the Nanos is 34x better than for the RPis. Comparing the Nanos against the VMs, we find η_e to be 10x, 50x, 59x, and 57x higher on the Nanos. For FEMNIST, the Nanos are 7x more energy efficient while for Shakespeare η_e is 34x higher.

We also find the Nanos to be more energy efficient than the GPU. η_e is 3x, 3x, 2x, and 2x higher for the BLOND CNN, LSTM, ResNet, and DenseNet models, respectively. For training on FEMNIST, the Nanos yield a 1.5x higher η_e than the GPU while for Shakespeare η_e increases to 2.3x.

The Nanos are consistently the most energy-efficient device type in our experiments, which suggests wide adoption in edge computing environments in the near future. Also, our evaluation shows the importance of evaluating FL applications w.r.t. their effects on energy efficiency. To provide a holistic picture, we list associated hardware utilization statistics in Appendix C.2.

5.3 Robustness of FL Systems

Existing FL strategies are robust against client dropouts. For the models on the BLOND dataset, we identify FedYogi as the best-performing strategy across all client dropout levels (Table 1). However, we observe a diminishing accuracy with increasing client dropouts per training round. While the BLOND CNN and DenseNet accuracy drop by 8 percentage points from training without client failures to 50% client failure, the LSTM and ResNet models only lose 7 and 4 percentage points, respectively. For the CNN used on the FEMNIST dataset, both FedAvg and FedProx perform equally well without client dropouts. Yet, with client dropout levels of 10% and higher, FedAvg outperforms FedProx. Between training without client failure and 50% client failures during training rounds,

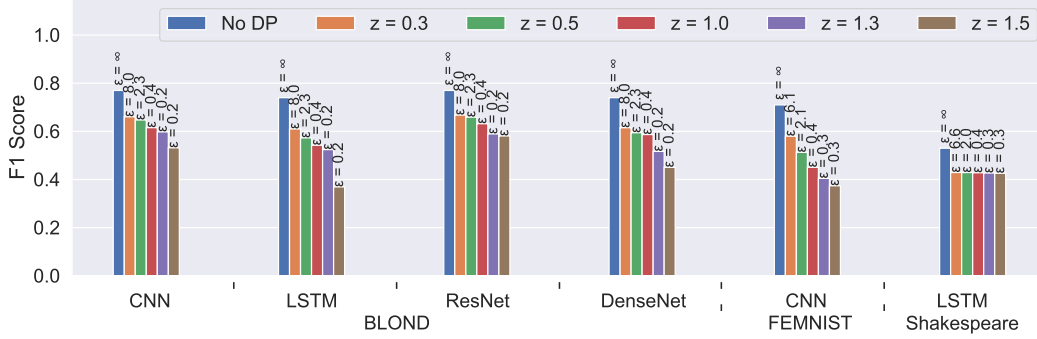


Figure 4: Results of various differential privacy levels (measured by the noise multiplier level z) across all non-IID datasets and models with the FedAvg FL strategy. The underlying dataset is identical to the dropout analysis. Labels above each bar report the privacy budget ϵ after ten rounds of training. DP experiments with other FL strategies are available in Appendix C.3

the accuracy only drops by 4 percentage points on the FEMNIST test dataset. The Shakespeare LSTM yields similar results as FEMNIST. Yet, without client dropouts FedAvg performs best. With client dropouts, FedAvg and FedProx are equally well suited for training, while the accuracy from 0% client dropouts to 50% only diminishes by 4 percentage points. As can be seen, FL strategies provide considerable robustness against client dropouts. Yet, their level of sensitivity toward dropouts differs. While we never achieve the highest accuracy with the qFedAvg strategy, it provides an equal or lower accuracy loss with increasing client dropout rates compared to the best-performing strategy. As such, the objective of introducing fairness with qFedAvg can also be achieved with client dropouts. The only exception is the FEMNIST CNN which never converged with qFedAvg in our experiments. Generally, we can conclude existing FL strategies have considerable robustness against client dropouts, yet with variability w.r.t. to the maximum accuracy.

There is no one strategy fits all solution. In our experiments, we see great variation in accuracy across FL strategies. Yet, for each dataset, there is exactly one strategy that outperforms all others. For all BLOND models, FedYogi is the best-performing strategy across dropout levels, being at least 4 percentage points better than all others in the 0% dropout bracket. For FEMNIST, FedAvg consistently performs best. Yet, with 0% client dropouts, FedProx is on-par. For Shakespeare, again, FedAvg is the best-performing strategy, while with increasing client dropout levels, FedProx gets on par with FedAvg. Our evaluations show the impact of careful FL strategy evaluation on training performance and, consequently, underpin the importance of hyperparameter optimization (HPO) on FL strategies. Approaches towards HPO in FL systems have been taken with FedHPO-B [5].

5.4 Differential Privacy

Tight privacy budgets come at a significant cost of accuracy. Training with the FedAvg strategy across all models, we observe an approx. 10 percentage points lower accuracy with noise multiplier $z = 0.3$ as compared to training without DP. The privacy budget spent for training the four BLOND models with $z = 0.3$ amounts to $\epsilon = 8$, which is considered a rather loose privacy budget [35], i.e., for practical utility, we would aim for a much lower ϵ . We achieve this by increasing the noise multiplier. By doing so, we find the BLOND CNN’s accuracy to continuously diminish. Yet, with $z = 1.3$, we observe $\epsilon = 0.2$; the same privacy budget we would get with $z = 1.5$. As such, it does not make sense to use $z > 1.3$. For BLOND LSTM, we observe a similar pattern, while there is almost a plateau between $1 \leq z \leq 1.3$, which does allow us to maintain tighter privacy budgets while achieving the same performance. However, for $z = 1.5$ we see a significant accuracy drop for the BLOND LSTM. Opposed, the ResNet model loses 10 percentage points in accuracy from $z = 0.3$ to $z = 1.5$ with a plateau between $1.3 \leq z \leq 1.5$. Yet, with $\epsilon = 0.2$, we already achieve the tightest privacy budget at $z = 1.3$. The DenseNet model has an accuracy plateau between $0.5 \leq z \leq 1$, while ϵ is 6x tighter. With higher noise multipliers the performance degrades significantly. For the FEMNIST CNN, we see a significant accuracy loss as the noise multiplier increases, while for the Shakespeare LSTM, we do not find a significant effect on the accuracy when increasing z .

We conclude from our experiments that achieving tight privacy guarantees may come at a significant cost of accuracy. However, for many models, there are only minor differences in accuracy between noise multiplier levels that may make a difference between tight and very tight privacy budgets, as can be seen with the BLOND LSTM, ResNet, and DenseNet models. (ϵ, δ) -DP can be a powerful tool against attack vectors on DL models [22, 23]. Additionally, we identify a minimum achievable ϵ on all DL models in our configuration. Beyond these ϵ it does not make sense to further increase the noise multiplier level. For designing private and secure FL systems the correct estimation of z is an integral decision criterion, as high noise levels have a substantial impact on training performance.

6 Conclusion

In this work, we introduce FLEdge, a modular benchmark for evaluating FL applications in edge computing systems. We show the computational limits of different embedded devices, evaluate their energy efficiency, and find that embedded devices are up to 3x more energy efficient than server-grade hardware, which in related work were frequently used to evaluate FL applications. We also outline the practical benefits of adopting hardware acceleration in edge computing systems, especially w.r.t. industrial applications. Additionally, our experiments show that the best-performing FL strategy highly depends on the DL task at hand. For each dataset, we identify one consistently best-performing strategy. This underpins the importance of carefully evaluating tasks on an individual basis. Our evaluation of user-level (ϵ, δ) -DP has shown that DP generally comes at a considerable cost of lower accuracy, yet the effects depend on the DL model used for a workload.

In summary, we show the importance of addressing FL challenges for edge computing systems holistically by evaluating new methods not only for training performance w.r.t. accuracy but also for applications in resource-constrained environments. We hope to spur more research toward FL methods optimized for edge computing.

Acknowledgments and Disclosure of Funding

This work is partially funded by the German Federal Ministry of Economic Affairs and Climate Action through ZIM (Zentrales Innovationsprogramm Mittelstand). Grant: 16KN085729.

References

- [1] Sebastian Caldas, Sai Meher Karthik Duddu, Peter Wu, Tian Li, Jakub Konečný, H. Brendan McMahan, Virginia Smith, and Ameet Talwalkar. Leaf: A benchmark for federated settings, 2018. URL <https://arxiv.org/abs/1812.01097>.
- [2] Chaoyang He, Songze Li, Jinhyun So, Xiao Zeng, Mi Zhang, Hongyi Wang, Xiaoyang Wang, Praneeth Vepakomma, Abhishek Singh, Hang Qiu, Xinghua Zhu, Jianzong Wang, Li Shen, Peilin Zhao, Yan Kang, Yang Liu, Ramesh Raskar, Qiang Yang, Murali Annavaram, and Salman Avestimehr. Fedml: A research library and benchmark for federated machine learning, 2020. URL <https://arxiv.org/abs/2007.13518>.
- [3] Fan Lai, Yinwei Dai, Sanjay S. Singapuram, Jiachen Liu, Xiangfeng Zhu, Harsha V. Madhyastha, and Mosharaf Chowdhury. FedScale: Benchmarking model and system performance of federated learning at scale. 2021. doi: 10.48550/ARXIV.2105.11367. URL <https://arxiv.org/abs/2105.11367>.
- [4] Daoyuan Chen, Dawei Gao, Weirui Kuang, Yaliang Li, and Bolin Ding. pfl-bench: A comprehensive benchmark for personalized federated learning, 2022. URL <https://arxiv.org/abs/2206.03655>.
- [5] Zhen Wang, Weirui Kuang, Ce Zhang, Bolin Ding, and Yaliang Li. Fedhpo-b: A benchmark suite for federated hyperparameter optimization, 2022. URL <https://arxiv.org/abs/2206.03966>.
- [6] Blesson Varghese, Nan Wang, Sakil Barbhuiya, Peter Kilpatrick, and Dimitrios S. Nikolopoulos. Challenges and opportunities in edge computing. In *2016 IEEE International Conference on Smart Cloud (SmartCloud)*. IEEE, November 2016. doi: 10.1109/smartcloud.2016.18. URL <https://doi.org/10.1109/smartcloud.2016.18>.
- [7] Xiaofan He, Juan Liu, Richeng Jin, and Huaiyu Dai. Privacy-aware offloading in mobile-edge computing. In *GLOBECOM 2017 - 2017 IEEE Global Communications Conference*. IEEE, December 2017. doi: 10.1109/glocom.2017.8253985. URL <https://doi.org/10.1109/glocom.2017.8253985>.
- [8] Jinke Ren, Guanding Yu, Yinghui He, and Geoffrey Ye Li. Collaborative cloud and edge computing for latency minimization. *IEEE Transactions on Vehicular Technology*, 68(5):5031–5044, May 2019. doi: 10.1109/tvt.2019.2904244. URL <https://doi.org/10.1109/tvt.2019.2904244>.
- [9] Najmul Hassan, Saira Gillani, Ejaz Ahmed, Ibrar Yaqoob, and Muhammad Imran. The role of edge computing in internet of things. *IEEE Communications Magazine*, 56(11):110–115, November 2018. doi: 10.1109/mcom.2018.1700906. URL <https://doi.org/10.1109/mcom.2018.1700906>.
- [10] Edge Networking | Dell USA, 2023. URL <https://www.dell.com/en-us/shop/servers-storage-networking/sf/access-platforms>.
- [11] Industrial Edge Devices, 2023. URL <https://www.siemens.com/global/en/products/automation/topic-areas/industrial-edge/industrial-edge-devices.html>.
- [12] Chao Li, Yushu Xue, Jing Wang, Weigong Zhang, and Tao Li. Edge-oriented computing paradigms. *ACM Computing Surveys*, 51(2):1–34, April 2018. doi: 10.1145/3154815. URL <https://doi.org/10.1145/3154815>.
- [13] Mohammad Goudarzi, Marimuthu Palaniswami, and Rajkumar Buyya. Scheduling IoT applications in edge and fog computing environments: A taxonomy and future directions. *ACM Computing Surveys*, 55(7):1–41, December 2022. doi: 10.1145/3544836. URL <https://doi.org/10.1145/3544836>.
- [14] Nvidia.com. Nvidia jetson agx orin series, 2022. URL <https://www.nvidia.com/content/dam/en-zz/Solutions/gtc21/jetson-orin/nvidia-jetson-agx-orin-technical-brief.pdf>.
- [15] Jetson Roadmap, February 2020. URL <https://developer.nvidia.com/embedded/develop/roadmap>.
- [16] Aritra Mitra, Rayana Jaafar, George J. Pappas, and Hamed Hassani. Linear convergence in federated learning: Tackling client heterogeneity and sparse gradients. In M. Ranzato, A. Beygelzimer, Y. Dauphin, P.S. Liang, and J. Wortman Vaughan, editors, *Advances in Neural Information Processing Systems*, volume 34, pages 14606–14619. Curran Associates, Inc., 2021. URL https://proceedings.neurips.cc/paper_files/paper/2021/file/7a6bda9ad6ffdac035c752743b7e9d0e-Paper.pdf.

- [17] Karan Singhal, Hakim Sidahmed, Zachary Garrett, Shanshan Wu, John Rush, and Sushant Prakash. Federated reconstruction: Partially local federated learning. In M. Ranzato, A. Beygelzimer, Y. Dauphin, P.S. Liang, and J. Wortman Vaughan, editors, *Advances in Neural Information Processing Systems*, volume 34, pages 11220–11232. Curran Associates, Inc., 2021. URL https://proceedings.neurips.cc/paper_files/paper/2021/file/5d44a2b0d85aa1a4dd3f218be6422c66-Paper.pdf.
- [18] Xiuwen Fang and Mang Ye. Robust federated learning with noisy and heterogeneous clients. In *Proceedings of the IEEE/CVF Conference on Computer Vision and Pattern Recognition (CVPR)*, pages 10072–10081, June 2022.
- [19] Daniel J. Beutel, Taner Topal, Akhil Mathur, Xinchu Qiu, Javier Fernandez-Marques, Yan Gao, Lorenzo Sani, Kwing Hei Li, Titouan Parcollet, Pedro Porto Buarque de Gusmão, and Nicholas D. Lane. Flower: A friendly federated learning research framework, 2020. URL <https://arxiv.org/abs/2007.14390>.
- [20] Intel. Intel xeon cpu max series. URL <https://www.intel.com/content/www/us/en/products/details/processors/xeon/max-series.html>.
- [21] Arm. Iot markets – internet of things markets. URL <https://www.arm.com/markets/iot>.
- [22] Milad Nasr, Reza Shokri, and Amir Houmansadr. Comprehensive privacy analysis of deep learning: Passive and active white-box inference attacks against centralized and federated learning. In *2019 IEEE Symposium on Security and Privacy (SP)*. IEEE, May 2019. doi: 10.1109/sp.2019.00065. URL <https://doi.org/10.1109/sp.2019.00065>.
- [23] Mohammad Naseri, Jamie Hayes, and Emiliano De Cristofaro. Local and central differential privacy for robustness and privacy in federated learning. 2020. doi: 10.48550/ARXIV.2009.03561. URL <https://arxiv.org/abs/2009.03561>.
- [24] Thomas Kriechbaumer, Anwar Ul Haq, Matthias Kahl, and Hans-Arno Jacobsen. MEDAL. In *Proceedings of the Eighth International Conference on Future Energy Systems*. ACM, May 2017. doi: 10.1145/3077839.3077844. URL <https://doi.org/10.1145/3077839.3077844>.
- [25] C. P. Kruger and G. P. Hancke. Benchmarking internet of things devices. In *2014 12th IEEE International Conference on Industrial Informatics (INDIN)*. IEEE, July 2014. doi: 10.1109/indin.2014.6945583. URL <https://doi.org/10.1109/indin.2014.6945583>.
- [26] Jonathan McChesney, Nan Wang, Ashish Tanwer, Eyal de Lara, and Blesson Varghese. DeFog. In *Proceedings of the 4th ACM/IEEE Symposium on Edge Computing*. ACM, November 2019. doi: 10.1145/3318216.3363299. URL <https://doi.org/10.1145/3318216.3363299>.
- [27] Blesson Varghese, Nan Wang, David Bermbach, Cheol-Ho Hong, Eyal De Lara, Weisong Shi, and Christopher Stewart. A survey on edge performance benchmarking. *ACM Computing Surveys*, 54(3):1–33, April 2022. doi: 10.1145/3444692. URL <https://doi.org/10.1145/3444692>.
- [28] Yuyi Mao, Changsheng You, Jun Zhang, Kaibin Huang, and Khaled B. Letaief. A survey on mobile edge computing: The communication perspective. *IEEE Communications Surveys & Tutorials*, 19(4):2322–2358, 2017. doi: 10.1109/comst.2017.2745201. URL <https://doi.org/10.1109/comst.2017.2745201>.
- [29] Yingchun Wang, Jingyi Wang, Weizhan Zhang, Yufeng Zhan, Song Guo, Qinghua Zheng, and Xuanyu Wang. A survey on deploying mobile deep learning applications: A systemic and technical perspective. *Digital Communications and Networks*, 8(1):1–17, February 2022. doi: 10.1016/j.dcan.2021.06.001. URL <https://doi.org/10.1016/j.dcan.2021.06.001>.
- [30] Jiasi Chen and Xukan Ran. Deep learning with edge computing: A review. *Proceedings of the IEEE*, 107(8):1655–1674, August 2019. doi: 10.1109/jproc.2019.2921977. URL <https://doi.org/10.1109/jproc.2019.2921977>.
- [31] D. Steinkraus, I. Buck, and P.Y. Simard. Using GPUs for machine learning algorithms. In *Eighth International Conference on Document Analysis and Recognition (ICDAR'05)*. IEEE, 2005. doi: 10.1109/icdar.2005.251. URL <https://doi.org/10.1109/icdar.2005.251>.
- [32] Andrew G. Howard, Menglong Zhu, Bo Chen, Dmitry Kalenichenko, Weijun Wang, Tobias Weyand, Marco Andreetto, and Hartwig Adam. Mobilenets: Efficient convolutional neural networks for mobile vision applications, 2017. URL <https://arxiv.org/abs/1704.04861>.
- [33] H. Brendan McMahan, Eider Moore, Daniel Ramage, Seth Hampson, and Blaise Agüera y Arcas. Communication-efficient learning of deep networks from decentralized data. *arXiv*, 2016. doi: 10.48550/ARXIV.1602.05629. URL <https://arxiv.org/abs/1602.05629>.

- [34] H. Brendan McMahan, Daniel Ramage, Kunal Talwar, and Li Zhang. Learning differentially private recurrent language models, 2017. URL <https://arxiv.org/abs/1710.06963>.
- [35] Galen Andrew, Om Thakkar, H. Brendan McMahan, and Swaroop Ramaswamy. Differentially private learning with adaptive clipping, 2019. URL <https://arxiv.org/abs/1905.03871>.
- [36] Kang Wei, Jun Li, Ming Ding, Chuan Ma, Howard H. Yang, Farokhi Farhad, Shi Jin, Tony Q. S. Quek, and H. Vincent Poor. Federated learning with differential privacy: Algorithms and performance analysis, 2019. URL <https://arxiv.org/abs/1911.00222>.
- [37] Cynthia Dwork and Aaron Roth. The algorithmic foundations of differential privacy. *Foundations and Trends® in Theoretical Computer Science*, 9(3-4):211–407, 2013. doi: 10.1561/04000000042. URL <https://doi.org/10.1561/04000000042>.
- [38] René Schwermer, Jonas Buchberger, Ruben Mayer, and Hans-Arno Jacobsen. Federated office plug-load identification for building management systems. In *Proceedings of the Thirteenth ACM International Conference on Future Energy Systems*, New York, NY, USA, June 2022. ACM.
- [39] Sashank Reddi, Zachary Charles, Manzil Zaheer, Zachary Garrett, Keith Rush, Jakub Konečný, Sanjiv Kumar, and H. Brendan McMahan. Adaptive federated optimization, 2020. URL <https://arxiv.org/abs/2003.00295>.
- [40] Tian Li, Anit Kumar Sahu, Manzil Zaheer, Maziar Sanjabi, Ameet Talwalkar, and Virginia Smith. Federated optimization in heterogeneous networks, 2018. URL <https://arxiv.org/abs/1812.06127>.
- [41] Tian Li, Maziar Sanjabi, Ahmad Beirami, and Virginia Smith. Fair resource allocation in federated learning, 2019. URL <https://arxiv.org/abs/1905.10497>.
- [42] IEEE standard for information technology– local and metropolitan area networks– specific requirements– part 3: CSMA/CD access method and physical layer specifications amendment 3: Data terminal equipment (DTE) power via the media dependent interface (MDI) enhancements. URL <https://doi.org/10.1109/ieeestd.2009.5306743>.
- [43] William Falcon et al. Pytorch lightning. *GitHub. Note: <https://github.com/PyTorchLightning/pytorch-lightning>*, 3(6), 2019.
- [44] Guillaume Fieni, Romain Rouvoy, and Lionel Seiturier. SelfWatts: On-the-fly selection of performance events to optimize software-defined power meters. In *2021 IEEE/ACM 21st International Symposium on Cluster, Cloud and Internet Computing (CCGrid)*. IEEE, May 2021. doi: 10.1109/ccgrid51090.2021.00042. URL <https://doi.org/10.1109/ccgrid51090.2021.00042>.
- [45] Karim Said Barsim, Roman Streubel, and Bin Yang. Unsupervised adaptive event detection for building-level energy disaggregation. *Proceedings of Power and Energy Student Summit (PESS), Stuttgart, Germany*, 2014.
- [46] Aug 2022. URL <https://developer.nvidia.com/blog/maxwell-most-advanced-cuda-gpu-ever-made/>.

Appendix

Due to the space limitation in the main paper, we provide additional details about experiment results, implementation, and reproducibility in this appendix. The appendix is structured as follows. We first explain details on the parameterization of our DL models. Second, we will provide additional information about our implementation and testbed. Third and finally, we will provide additional experiment results on different data distributions and differentially private workloads.

Appendix A Dataset & Model Parameterization

In this section, we describe the exact parameterization for reproducing our experiment results.

A.1 Datasets

We use three publicly available datasets in our benchmark. Each dataset is widely used in its field of application for exploring FL. We describe essential properties of each dataset in Table 2. All datasets are sampled from a Dirichlet distribution with $\alpha = 1$ for 45 clients to match our testbed size. All datasets can be downloaded from our cloud repository.⁴ Yet, FLEdge is easily extensible with additional datasets (see details in Appendix B), which allows for quick adoption to further domains.

Table 2: DL pipelines employed in our evaluations

| Pipeline | Dataset Name | Total Samples | Samples per Device | Format | Size |
|----------|--------------|---------------|--------------------|--------|---------|
| NILM | BLOND | 13,164 | 234±132 | HDF5 | 5.46 GB |
| CV | FEMNIST | 814,255 | 13,958±2,106 | PNG | 3.34 GB |
| NLP | Shakespeare | 4,226,054 | 75,131±18,281 | TXT | 0.38 GB |

BLOND. BLOND is a dataset capturing electrical appliances in building-level office environments, such as laptops, monitors, and printers. In total, the dataset consists of 12 classes. We adopt Schwermer et al.’s [38] approach to FL with BLOND. Each sample in the dataset consists of 25,600 power readings (current, voltage). Instead of generating the input features for the DL models in the data loader, we deviate from Schwermer et al. and create the Active Power, Apparent Power, Reactive Power, and MFCC ($n_mfcc = 64$) input features offline [45]. This results in a sample size of 68×1 . The main reason is to reduce dataset size in order to fit the dataset onto our RPi devices. Exact details on data preprocessing are available in our code.

FEMNIST. For CV, we adopt the FEMNIST dataset with a by-class categorization as introduced by Caldas et al. [1]. The FEMNIST dataset contains 62 classes of handwritten digits (26 lower case letters, 26 upper case letters, and 10 digits). We random crop the gray scale samples to 28×28 and perform a random flip before training.

Shakespeare. To explore NLP applications, we opt for the widely used Shakespeare dataset [1, 2]. It consists of the complete works of William Shakespeare. It is preprocessed in the exact same way as introduced in the LEAF benchmark [1]. The dataset was preprocessed with a sliding window of 80 characters and a stride of 1 to prepare it for the next-character prediction task. The vocabulary was generated over all the alphabet including special characters resulting in a total size of 80.

A.2 DL Models

BLOND. We align with the existing work by Schwermer et al. [38] and adopt their models for our evaluations. Specifically, the CNN consists of one convolutional layer with a 3×1 kernel and a padding of 1 as well as one fully connected layer with an output dimension of 12. The LSTM model contains one LSTM layer with a hidden size of 15 followed by a fully connected linear layer. The ResNet model consists of five layers; four of which are ResNet-inspired with a hidden size of 28 and a skip connection, followed by a fully connected layer. The five-layer DenseNet architecture is inspired by the DenseNet reference architecture with a hidden size of 32 and the fifth layer being a

⁴https://syncandshare.lrz.de/getlink/fi8NCT2xSFPnzkuVdDoN8D/presampled_45_clients(Link does not track access or download statistics)

Table 3: DL model hyperparameters

| Dataset | Model | Optim. | LR | W. Decay | Dropout | Hidden Dim | Params | Minibatch |
|-------------|----------|--------|-------|----------|---------|------------|---------|-----------|
| BLOND | CNN | SGD | 0.055 | 0.0 | | | 14,000 | 128 |
| | LSTM | SGD | 0.045 | 0.001 | 0 | 15 | 40,000 | 128 |
| | ResNet | SGD | 0.052 | 0.001 | | | 100,000 | 128 |
| | DenseNet | SGD | 0.075 | 0.001 | | | 252,000 | 128 |
| FEMNIST | CNN | Adam | 0.001 | 0.0 | | | 33,000 | 32 |
| Shakespeare | LSTM | SGD | 0.8 | 0.0 | 0 | 256 | 819,000 | 32 |

fully connected layer. For all models we use ReLU activations. For the exact implementation please refer to our code base, specifically to `pipelines/blond/models.py`.

FEMNIST. For FEMNIST, we use a two-layer CNN. Both convolutional layers have a 5x5 kernel. The first and second layer have 6 and 12 output dimensions, respectively. Each layer is followed by a max pooling layer with kernel 2x2 and stride 2. The convolutions are followed by two fully connected layers with a size of 192 and 120, respectively. All layers have a ReLU activation function. For the exact implementation please refer to our code base, specifically to `pipelines/mnist/models.py`.

Shakespeare. The embedding contains a vocabulary of 80 and has 8 dimensions. The two LSTM layers each have a hidden size of 256. It is followed by a sequential layer that has an output dimension of 80, equal to the vocabulary size to predict the next character. For the exact implementation please refer to our code base, specifically to `pipelines/shakespeare/models.py`.

A.3 FL Strategies

Below we elaborate on all six FL strategies used in our work and their parameterization. Details on the exact parameterization of every FL strategy can be found in Table 4.

Table 4: FL strategy hyperparameters. Key: η , η_l = server-side learning rates, β_1 , β_2 = Weight decay rates, τ = Server-side adaptivity level, q = Fairness parameter for qFedAvg, μ = proximal parameter for FedProx.

| FL Strategy | Dataset | η | η_l | β_1 | β_2 | τ | q | μ | Further Details |
|-------------|-------------|--------|----------|-----------|-----------|-----------|-----------|-----------|---|
| FedAvg | All | - | - | - | - | - | - | - | FedAvg does not have any server hyperparameters |
| FedAdam | All | -1.5 | -1 | 0.9 | 0.99 | $1e^{-2}$ | - | - | |
| FedAdaGrad | All | 0 | 0 | - | - | $1e^{-3}$ | - | - | |
| FedYogi | All | -1.5 | -1.5 | 0.9 | 0.99 | $1e^{-5}$ | - | - | |
| FedProx | Shakespeare | - | - | - | - | - | - | $1e^{-2}$ | |
| | Others | - | - | - | - | - | - | 1 | |
| qFedAvg | Shakespeare | - | - | - | - | - | $1e^{-2}$ | - | |
| | Others | - | - | - | - | - | 1 | - | |

FedAvg. FedAveraged Averaging aggregated model updates based on a weighted average over the number of samples clients contribute to the learning process [33]. FedAvg does not have any hyperparameters.

FedOpt (FedAdam, FedYogi, FedAdaGrad). Reddi et al. [39] introduce adaptive FL strategies with server-side learning rate and weight decay to better account for client heterogeneity. Yet, the server-side hyperparameters increase complexity w.r.t. optimizing the training process. We follow the authors and adapt their FL strategy hyperparameters for our experiments.

FedProx. With FedProx, Li et al. [40] account for client heterogeneity w.r.t. to their compute performance by allowing partial model updates. They modify FedAvg with a proximal μ , which aims to reduce divergence of local models on clients from the global model and respect partial updates coming from stragglers. For our experiments, we parameterize FedProx as proposed by Li et al. [40].

qFedAvg. Li et al. [41] introduce q-fair FedAvg a FL strategy to increase overall fairness and improve generalizability of a global DL model. This is done by overweighting clients that have a

higher loss compared to others. q determines the degree of overweighting clients. Yet, the authors note that finding q must be done on a case-by-case basis, i.e., by trying out different q 's. For our work, we adopt the suggested $q = 0.001$ for Shakespeare and use $q = 1$ for the other datasets.

Appendix B Implementation & Testbed Details

We implement FLEdge on top of a widely used software stack for FL applications. The source code of FLEdge is available on <https://github.com/laminair/FLEdge> including all dependencies and instructions for installation. We based our implementation on Flower to provide easy extensibility with new FL strategies and ML pipelines. We further provide scripts to sample datasets IID and Dirichlet non-IID.

Table 5: Software Stack

| Type | Name | Version | Details |
|----------------------|-------------------|-----------|---|
| Operating System | Ubuntu | 20.04 LTS | |
| Implementation Basis | Python | 3.9 | |
| ML Library | PyTorch | 1.10.1 | We use PyTorch in conjunction with CUDA & cuDNN where applicable. CUDA & cuDNN versions are the latest versions for the corresponding platform. |
| ML Framework | PyTorch Lightning | 1.5.10 | Used to improve extensibility. |
| FL Framework | Flower | 0.18.0 | |
| Logger Service | Weights & Biases | 0.13.1 | |

B.1 Device Configurations

Since we use different device types, there are various important specifications to reproduce our benchmark results. We aimed to use the latest available platform on all devices with long-term support (LTS).

NVIDIA Jetson Nano 2GB. Our Jetsons are running on NVIDIA JetPack 4.6. This includes Ubuntu 18.04 LTS with Python 3.6, and PyTorch 1.10.⁵ The latest supported CUDA version is 10.2 with cuDNN 7.2. We use Class 10 SD cards with 128 GB of storage. The Nanos are connected via 1 GBit/s PoE+ [42] and can draw up to 15 Watt peak power.

Raspberry Pi 4B. We use RPi 4B with 4GB of memory in our experiments. They are running with Ubuntu 20.04 LTS, Python 3.9, and PyTorch 1.10. There is no hardware acceleration available. The RPis are equipped with a class 10 32 GB SD card each and have a 1GBit/s network interface. The RPis have a peak power draw of 10 Watts.

x86 Desktop Clients. We emulate small desktop clients with an x86-CPU via our private cloud. Each VM has 4 CPU cores and 4 GB of memory with 30 GB SSD storage. The VMs have a 1 GBit/s network link. We use Ubuntu 20.04 LTS with Python 3.9 and PyTorch 1.10. We use the estimates from SelfWatts [44] as the power utilization profile for each VM. Fieni et al. calculate approx. 50 Watts for a 4 CPU core VM on Intel Xeon E5 processors.

GPU. As a GPU server, we use a VM with 64 x86-CPU cores and 256 GB of memory with an NVIDIA RTX A6000 GPU (PCI passthrough, non-virtualized). The VM has 3 TB NVMe storage. The VM is running Ubuntu 20.04 LTS with Python 3.9 and PyTorch 1.10. We use CUDA 11.6 and cuDNN 8.6.

B.2 Details on Energy Monitoring

Our testbed is built with a focus on the measurability of as many aspects as possible, including power draw and energy. Therefore, we use PoE+ switches for all embedded devices. Each device gets a full 1000 MBit/s network connection (adjustable to 10, 100, and 1000 MBit/s). The switches allow monitoring of energy metrics with 1 Hz. We use a PostgreSQL DB to capture the energy metrics for

⁵The latest platform supported on the Jetson Nanos is JetPack 4.6 (Ubuntu 18.04 LTS, Python 3.6, PyTorch 1.10, CUDA 10.2). The Maxwell architecture was released in 2014 [46].

each embedded device. The DB has an interface that allows each embedded device to read its own power statistics in real-time.

Appendix C Additional Experiment Results

Due to space limitations, we provide additional experimental results in this section. They support our main findings in the paper. We investigate the training performance across three datasets and six DL models by measuring the training time and energy consumption.

C.1 Hardware Heterogeneity

To address hardware heterogeneity, we present a micro-benchmark measuring all steps required to train DL models. In the following, we describe each step in more detail. Table 6 shows detailed speed comparisons between the four device classes used in our work.

Batch Loading. With this, we measure the time it takes to load one minibatch of data from the disk into memory. This also includes the CUDA move time, in case we are working with GPUs. Ultimately, a major factor is the used storage medium, e.g., SD cards in embedded devices or NVMe storage in GPU-accelerated servers.

Forward Step. We measure the time it takes for a minibatch to be processed by the DL model. The timing is also relevant for inference profiling.

Loss Calculation. The time it takes to compare the model outputs to the ground truth labels. During our experiments, we never found timing spikes for the loss calculation step.

Backward Step. The backward step calculates the effect each model weight had on the predicted output. It plays a subordinate role in all models discussed in this paper.

Optimizer Step. After each processed minibatch, the optimizer step applies the calculated gradients onto the model weights to reduce the prediction error.

C.2 Energy Efficiency

To provide a full picture of energy efficiency, we provide additional metrics on hardware utilization in Table 7. For each dataset, DL mode, and device type we report the CPU, Memory, and GPU utilization. Furthermore, we provide the average power draw over the experiment duration.

CPU. The CPU statistics are averaged over one, five, and 15 minutes to provide an intuition of how much resources experiments use in the short, mid, and long term (in the context of FL workloads).

Memory. We report the average memory utilization of the entire system along with the memory utilization of the DL training process on each device.

GPU. For the GPU, we report the average utilization along with the VRAM allocation during our experiments. For The NVIDIA Jetson Nanos we cannot report memory allocation as the memory is shared between CPU and GPU.

Power. We measure the average power draw per experiment. Please note that the VM’s power consumption is an approximation we have taken from SelfWatts [44], who run experiments on VMs that match our specifications.

C.3 Differential Privacy

In this section we complement the experiments from Section 5.4 and report the training performance of FedAdam, FedAdaGrad, FedYogi, FedProx, and qFedAvg with various degrees of user-level (ϵ, δ) -DP (Figure 5). It is noteworthy, that the FL strategies respond similar to DP as compared to FedAvg, which we discuss in the main paper. However, the only difference is qFedAvg, which aims at increasing fairness in a systems. Therefore, the level of fairness (denoted with q) we chose generally causes the DL models either converge at a significantly lower accuracy or to not converge at all (Figure 5e). This resonates from clients with high loss as their updates are overweighted as per q . The effects are especially strong for the BLOND DenseNet and the FEMNIST CNN models. Also,

the Shakespeare LSTM shows significant sensitivity towards increasing levels of DP, which is not observable when experimenting with other FL strategies.

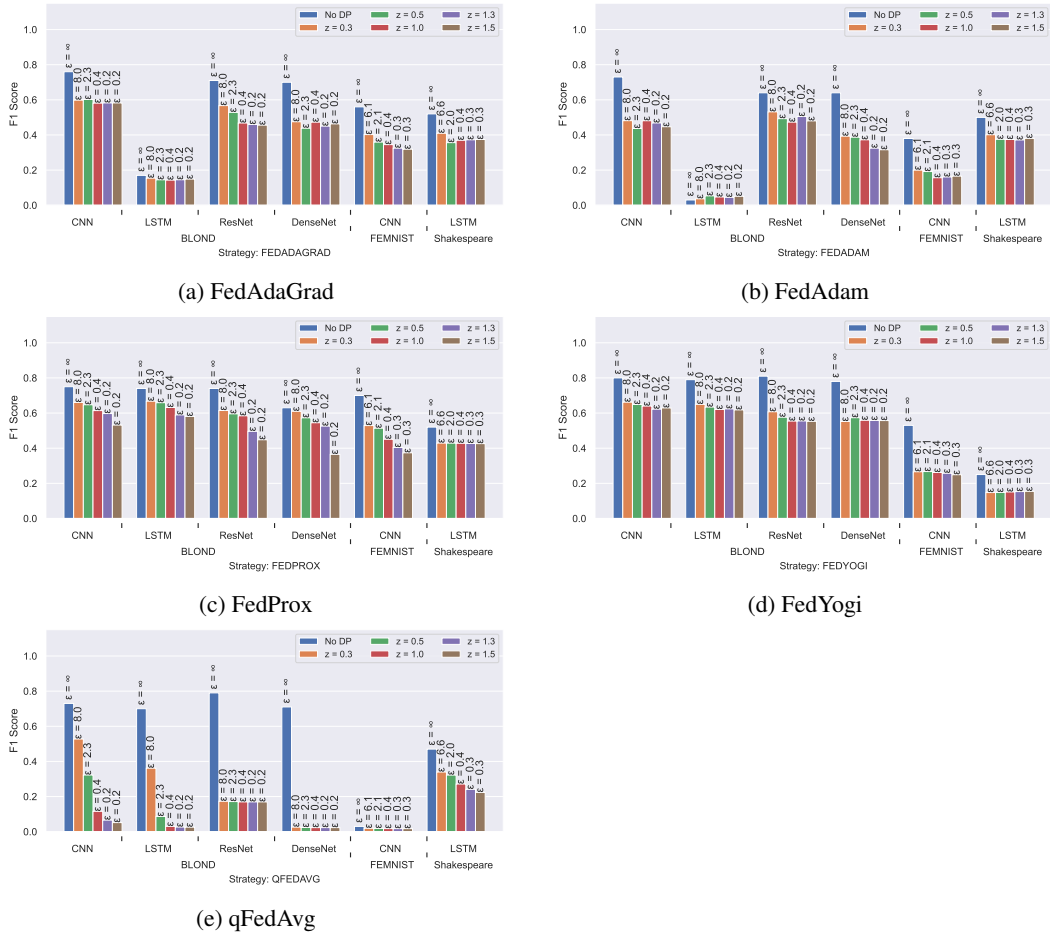


Figure 5: We complement Section 5.4 with additional (ϵ, δ) -DP experiments. We use all FL strategies, datasets (non-IID), and DL models discussed in our paper.

Table 7: System metrics for our energy efficiency experiments. We report CPU, memory, and GPU utilization. Note: The Nanos do not have dedicated VRAM as they are an SoC. As such, we cannot report GPU memory statistics.

| Dataset | Model | Device | CPU Util. Avg. (%) | | | Memory (MB) | | GPU | | |
|-------------|----------|--------|--------------------|--------|---------|-------------|-----------|-----------|-------------|-----------|
| | | | 01-min | 05-min | 15-min | Process | Total | Util. (%) | Memory (MB) | Power (W) |
| BLOND | CNN | GPU | 4±3 | 3±1 | 2±1 | 589±2 | 4027±1720 | 1±0 | 14±30 | 61±5 |
| | | VM | 60±32 | 67±31 | 67±34 | 554±106 | 1686±784 | | | 50±0 |
| | | Nano | 73±20 | 69±19 | 69±22 | 884±222 | 1724±226 | 84±17 | N/A | 5±1 |
| | | RPi | 54±21 | 56±19 | 69±35 | 368±9 | 1156±350 | | | 6±1 |
| | DenseNet | GPU | 5±4 | 3±2 | 3±1 | 592±3 | 4014±1710 | 1±0 | 439±350 | 60±4 |
| | | VM | 71±26 | 76±24 | 77±24 | 717±103 | 2149±738 | | | 50±0 |
| | | Nano | 76±19 | 74±16 | 73±17 | 828±241 | 1740±204 | 93±22 | N/A | 5±1 |
| | | RPi | 84±21 | 82±10 | 78±8 | 542±61 | 1514±307 | | | 7±1 |
| | LSTM | GPU | 3±3 | 3±1 | 3±1 | 589±3 | 3972±1551 | 1±0 | 32±14 | 60±4 |
| | | VM | 69±29 | 73±28 | 70±31 | 554±113 | 2074±866 | | | 50±0 |
| | | Nano | 72±19 | 69±17 | 72±18 | 800±236 | 1701±240 | 87±12 | N/A | 5±1 |
| | | RPi | 45±13 | 51±9 | 68±25 | 388±22 | 1181±346 | | | 6±1 |
| ResNet | GPU | 3±2 | 3±1 | 3±1 | 591±2 | 3988±1721 | 1±0 | 393±262 | 61±4 | |
| | VM | 67±26 | 74±27 | 74±28 | 723±120 | 2031±712 | | | 50±0 | |
| | Nano | 75±21 | 73±18 | 72±17 | 846±225 | 1741±208 | 91±23 | N/A | 5±2 | |
| | RPi | 83±24 | 70±15 | 73±15 | 577±76 | 1548±317 | | | 7±1 | |
| FEMNIST | CNN | GPU | 5±1 | 4±1 | 3±1 | 681±8 | 5887±1186 | 4±1 | 94±73 | 75±6 |
| | | VM | 96±12 | 95±12 | 92±14 | 546±301 | 2423±693 | | | 50±0 |
| | | Nano | 93±14 | 93±13 | 92±13 | 645±140 | 1672±93 | 89±31 | N/A | 6±1 |
| | | RPi | 98±11 | 98±7 | 97±7 | 674±85 | 1974±354 | | | 6±1 |
| Shakespeare | LSTM | GPU | 3±1 | 3±0 | 3±0 | 454±1 | 7375±907 | 33±6 | 2621±738 | 93±5 |
| | | VM | 93±7 | 94±4 | 95±4 | 1856±452 | 3869±270 | | | 50±0 |
| | | Nano | 63±22 | 70±20 | 84±13 | 740±232 | 1731±207 | 98±14 | N/A | 5±2 |
| | | RPi | 77±17 | 92±5 | 100±0 | 424±22 | 1411±249 | | | 7±1 |